DOI: 10.1002/chem.201000453

# Localized Deposition of Au Nanoparticles by Direct Electron Transfer through Cellobiose Dehydrogenase

**Esteban Malel,[a] Roland Ludwig,[b] Lo Gorton,[c] and Daniel Mandler*[a]**

**Abstract:** Cellobiose dehydrogenase (CDH) is a fascinating extracellular fungal enzyme that consists of two domains, one carrying a flavin adenine dinucleotide (FAD) and the other a cytochrome-type heme b group as cofactors. The two domains are interconnected by a linker and electrons can shuttle from the FAD to the heme group by intramolecular electron transfer. Electron transfer between CDH and an electrode can occur by direct electron transfer (DET) and by mediated electron transfer (MET). This characteristic makes CDH an interesting candidate for integration in systems such as biosensors and biofuel cells. Moreover, it makes CDH an alternative for the reduction of metal ions through DET and MET. In this work we have explored the localized deposition of gold on Pd substrates by CDH through DET and MET. For this purpose we exploited the advantage of scanning electrochemical microscopy (SECM) as a patterning tool. We first demonstrated that gold nanoparticles can be formed in homogenous solution. Then we showed that Au nanoparticles can also be locally formed and deposited on surfaces through DET at low pH and by MET at neutral pH using benzoquinone/hydroquinone as mediator.

**Keywords:** biocatalysis · gold · electrochemistry · enzymes · nanoparticles

## Introduction

The formation and deposition of metallic nanoparticles encompasses a major part of the activity in nanochemistry and nanotechnology.[1, 2] The most common approach is reduction of metal ions such as $AuCl_4^-$ by a reducing agent in the presence of a stabilizing substance. The rate and conditions of the reduction process affect significantly the size and distribution of the nanoparticles. Nucleation and particle growth, which are the two principal processes in nanoparticle formation, are also influenced by the ratio between the metal ions and the reducing and stabilizing agents.[3]

The introduction of biomolecules has enabled biocatalyzed formation of nanoparticles with milder reductants under more benign conditions.[4] Different approaches have been applied.[5] For example, Wright and Sewell synthesized $TiO_2$ by using a peptide and poly(L-cysteine) to form 50 and 140 nm particles, respectively.[5b] Similarly, Stone and coworkers synthesized Ag nanocrystallites with different geometries.[5a] Different peptides were selected for silver reduction and precipitation on the basis of their ability to bind to the surface of silver particles and clusters. The ability of biomolecules to produce and attach inorganic nanoparticles to various surfaces has also been exploited and termed bio-enabling and biomimetic synthesis of nanoparticles.[6] For instance, Umetsu et al. immobilized flower-like ZnO structures onto gold using peptides. The affinity of the peptides to Au was increased by anchoring cysteine moieties, whereas glycine residues served as electron donors.[6d] An interesting approach was demonstrated by Tsukruk and co-workers for the deposition of inorganic nanoparticles using a layer-by-layer technique. This allowed controlled adsorption of different biomolecules which affected nucleation and growth of nanoparticles. For example, poly-L-tyrosine was adsorbed onto surfaces modified with poly(allylamine hydrochloride) and poly(4-styrenesulfonate) to form gold NPs encapsulated in the poly amino acid.[6a] Similarly, titania NPs were grown by recombinant silaffin molecules attached to a polyelectrolyte-modified substrate.[6b]

[a] E. Malel, Prof. Dr. D. Mandler
Department of Inorganic and Analytical Chemistry
The Hebrew University of Jerusalem
Jerusalem 91940 (Israel)
Fax: (+972) 26585319
E-mail: mandler@vms.huji.ac.il

[b] Dr. R. Ludwig
APART Recipient of the Austrian Academy of Sciences
at the Institute of Analytical Chemistry/Biochemistry
Lund University, P. O. Box 124, 221 00 Lund (Sweden)

[c] Prof. Dr. L. Gorton
Institute of Analytical Chemistry/Biochemistry
Lund University, P.O. Box 124, 221 00 Lund (Sweden)

   

Enzymes have also been used for the synthesis of metal nanoparticles.[7] For example, glucose oxidase (GOx) has been used to catalyze the oxidation of glucose to gluconic acid producing hydrogen peroxide. It served as a mild reducing agent to form and enlarge gold nanoparticles.[7d] In a similar study, Au nanoparticles were obtained upon oxidation of L-dopa, which was formed by hydroxylation of L-tyrosine catalyzed by tyrosinase. Furthermore, the change in the absorption spectrum of the nanoparticles allowed the detection of L-dopa and other neurotransmitters.[7a] In most of these studies, the reducing agent, for example, dopamine, was generated by an enzyme-catalyzed reaction.

Localized biocatalyzed metal deposition was reported by dip-pen nanolithography with GOx, galactose oxidase and other enzymes.[2a] Recently, Wang et al. used AFM tips modified with horseradish peroxidase to generate nanopatterns of conductive polymers.[8]

Our study takes advantage of scanning electrochemical microscopy (SECM) as a patterning tool. The main feature of SECM is its ability to generate a controlled flux of electroactive species close to an interface. This allows charge-transfer processes as well as electroactivity and morphology of the interface to be studied.[9]

SECM has also been widely used for micro- and nanopatterning.[1e,9e,10] Of particular relevance to this study is localized metal deposition, which has been explored by SECM in different approaches.[1e,10a–c,e,f,11] We recently described electroless deposition (ELD) of gold nanoparticles by SECM using hydroquinone ($H_2Q$) as reducing agent and Pd as a catalytic substrate.[10d] The approach involved anodic dissolution of a gold microelectrode close to a catalytic surface in the presence of $H_2Q$. In spite of the fact that localized ELD was successful, there is at least one major drawback to this approach. The potential applied to oxidize the gold microelectrode also oxidized $H_2Q$. Hence, a milder or kinetically more stable reductant that is not oxidized upon electrochemically generating a flux of $AuCl_4^-$ is preferred. This could be resolved using enzymes that would allow less reactive reductants, such as glucose, to be employed. Moreover, the mediator (e.g., $H_2Q$) which can be enzymatically generated could be added in catalytic concentration.[12] Finally, direct electron transfer (DET) between an enzyme and metal ions could completely eliminate the need for a mediator.[13]

Cellobiose dehydrogenase (CDH, E.C. 1.1.99.18) is the only known extracellular flavocytochrome of fungal origin and contains two domains: the catalytically active flavin domain (FAD, containing flavin adenine dinucleotide) and the heme domain (heme, carrying a cytochrome-type heme b). This enzyme, which was also known as flavoprotein cellobiose:quinone oxidoreductase (E.C. 1.1.5.1, deleted in 2002)[14] has been studied in detail.[14–15] The two domains are interconnected by an approximately 25-residue-long linker, which allows different ET pathways. Electron transfer to the final electron acceptor depends on the environment and on the conformation of the two domains in the protein. Gorton and co-workers found that electron transfer between CDH and an electrode could be achieved by DET and MET.[16] Cellobiose and other higher cellodextrins are oxidized to their corresponding lactones in the FAD domain by two-electron two-proton transfer with a proper mediator, that is, a two-electron two-proton acceptor such as benzoquinone (BQ).[13,16b] If a one-electron acceptor is available, electron transfer can occur also in the FAD domain or heme domain. This pathway requires internal electron transfer between the two enzyme domains. Besides cytochrome c, different electrodes have been used as one-electron acceptors[17] requiring the presence of a heme domain.[18] On graphite DET was observed and used as a biosensor for different substrates.[19] Direct ET was also achieved through interaction of self-assembled monolayers on an Au surface.[16b] In general, the ET path is primarily controlled by the pH and the enzyme source. Deprotonation of surface-exposed amino acid residues on both domains of CDH affects its conformation and increases the distance between the FAD and heme domains. As a result, the DET process diminishes and the addition of a mediator favours an MET process. Hence, at pH 5 and below, the preferred electron-transfer path is DET, while at pH 7 MET prevails.

This characteristic makes CDH attractive for integration in systems such as biosensors and biofuel cells, in which DET occurs between enzyme and the electrode.[12,17] Moreover, its properties make CDH an excellent candidate for reduction of metal ions through DET and MET.

In this work we explored the deposition of gold nanoparticles on Pd through DET and MET of CDH. We clearly demonstrate that gold nanoparticles can be formed in homogenous solution and locally deposited on surfaces through DET at low pH and by MET at neutral pH with benzoquinone/hydroquinone as mediator.

## Results and Discussion

**Enzymatic reduction of $AuCl_4^-$**: Enzymatic biocatalyzed deposition of gold was explored through two pathways (Figure 1). In the first approach (Figure 1A) CDH is used to regenerate a redox mediator, namely, hydroquinone

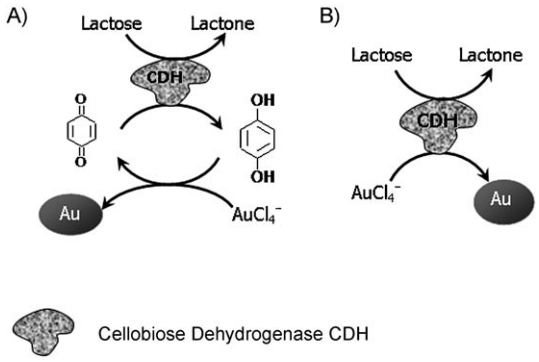


Figure 1. Schematics of biocatalyzed gold reduction. A) MET approach and B) DET approach.

  

($H_2Q$), which is consumed by reduction of $AuCl_4^-$ to Au catalyzed by a substrate.[10d] Therefore, the amount of $H_2Q$ needed for the reaction could, in principle, be reduced to catalytic levels. This MET process, namely, the biocatalyzed reduction of BQ, has already been exploited for biosensors,[12] but never as a source for depositing nanoparticles. As mentioned above, under proper conditions CDH could also participate in DET to carbon or gold electrodes. The location of the heme group in CDH facilitates oxidation of β-D-lactose by the FAD group and the transfer of electrons to the electrode. Metal ions could also be used as electron acceptors if they interact tightly with the heme group.[20] This would lead to the second approach (Figure 1B), in which a mediator is no longer needed.

We began by studying the first approach (Figure 1A), whereby formation of $H_2Q$ was monitored with a rotating disc electrode (RDE), which allows the homogeneous formation of $H_2Q$ in stirred solutions to be determined. The potential of 1.0 V applied to the gold electrode assured diffusion-controlled oxidation of enzymatically formed $H_2Q$. The substrate used in the experiments was β-D-lactose, and BQ was used as electron acceptor. Figure 2 shows the number of moles of $H_2Q$ oxidized as a function of time. The current and therefore the number of moles generated in the absence of CDH were negligible. The activity of the enzyme was studied at pH 5 and pH 7. Previous reports (vide supra) indicated that the mechanism of ET by CDH depends on pH and electron acceptor. At pH 7, DET is impossible because no electrons can be transferred from the FAD domain to the heme domain due to the lack of intramolecular electron transfer. From our experiments it is evident that $H_2Q$ is enzymatically formed and its formation is faster at pH 7 than at pH 5. The same amount of CDH was added in both experiments. The enzymatic activity was calculated from the initial slope of these curves. We found that CDH activity was $58.2 \pm 0.6$ and $25.8 \pm 0.2$ U mL$^{-1}$ for pH 7 and 5, respectively. Our findings, which show higher activity of CDH at elevated pH, are in accordance with the literature[13,17] and previous photometric measurements.[19a] At this pH internal ET between the two enzyme domains is almost shut off. Hence, electron transfer occurs solely through the FAD domain.

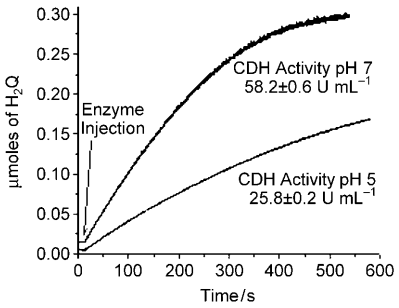


Figure 2. Amount of $H_2Q$ formed as a function of time measured by an RDE ($E = 1.0$ V vs. Ag|AgCl, rotation speed 1500 rpm) in 0.1 M phosphate buffer (pH 5 and 7) containing of 0.3 mM BQ, 0.3 mM lactose and 20 μL of CDH solution.

The enzymatically generated $H_2Q$ was further coupled to the reduction of $AuCl_4^-$ ions to form Au nanoparticles (NPs), formation of which was monitored spectroscopically (Figure 3). This reaction was studied by us recently,[10d] and

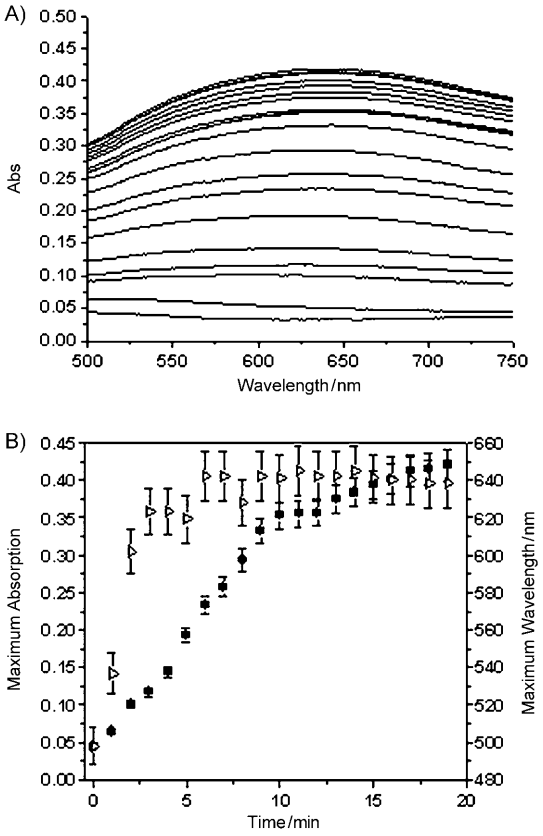


Figure 3. Gold nanoparticle absorption at pH 7. A) Absorption spectra of the reaction solution that contained 0.3 mM BQ, 0.3 mM β-D-lactose, 0.3 mM $HAuCl_4$ and 58.2 U mL$^{-1}$ CDH. Interval between runs 1 min. B) Absorption spectra as function of time showing the absorption maxima (●) and shift in maximum wavelength (▷).

we found that it required a catalyst, such as a Pd or Au surface, which dramatically enhanced the rate of $AuCl_4^-$ reduction. Furthermore, the size, shape and distribution of the nanoparticles were controlled by the pH of the solution. At pH 1–5, deposition was very fast and the deposit was dense due to fast nucleation and growth. At pH 6–7 the overall rate was sluggish, nuclei growth dominated and larger nanoparticles resulted.

Figure 3A shows the formation of Au NPs at pH 7. The solution contained BQ (0.3 mM), β-D-lactose (0.3 mM) and CDH (58.2 U mL$^{-1}$). The increase in absorption at 639 nm is due to the surface plasmon of Au NPs,[21] which corresponds to relatively large NPs with a size of 270 nm. No change in absorption was detected at 639 nm for BQ-free solution even after 3 h (not shown). This clearly implies that at pH 7 no DET between CDH and $AuCl_4^-$ took place. Hence, MET (Figure 1A) can be assumed for nanoparticle formation at pH 7. The broad absorption curve indicates wide NP

  

size distribution. Figure 3B shows a continuous increase in absorption and an almost constant maximum wavelength. These results suggest a continuous nucleation and growth mechanism for the formation of Au NPs.

It is somewhat surprising that Au NPs are formed in the absence of a catalytic surface. Control experiments conducted at pH 7 in the absence of gold nanoparticles and enzyme in a solution containing of $H_2Q$ (0.3 mM) and $AuCl_4^-$ (0.3 mM) resulted in the appearance of absorption at 570 nm due to the formation of Au NPs. We believe that at this pH the reducing potential of $H_2Q$ (which increases with pH[22]) is sufficient to reduce the gold salt (in the absence of a catalyst) and form a few gold clusters, which serve as catalytic sites for further reduction. The concentration of $H_2Q$ was relatively low, and it was not regenerated by the reduction of $AuCl_4^-$ (vide infra), and therefore the amount of Au NPs was limited by the initial concentration of $H_2Q$.

On the other hand, carrying out exactly the same experiment as described in Figure 3, but at pH 5, resulted in a negligible change of the spectrum (not shown). This is attributed to the driving force of $AuCl_4^-$ reduction by $H_2Q$ in solution, which decreases with increasing acidity. Interestingly, some Au NPs were formed when the experiment was performed in the absence of BQ at pH 5 (also not shown). This suggests that at pH 5, BQ competes for the flow of electrons that are generated by lactose oxidation. Yet, reduced BQ, namely, $H_2Q$, does not lead at this pH to efficient $AuCl_4^-$ reduction in the absence of a catalytic surface.

Hence, we carried out a series of experiments at pH 5 in the absence of BQ (Figure 4). The formation of Au NPs can clearly be seen in a solution consisting of lactose, CDH and Au NPs. Furthermore, the continuous increase in the absorption is correlated also with a red-shift of the maxima (Figure 4B). Both the increase of absorption and the shift of wavelength vary almost linearly with time. This indicates that $AuCl_4^-$ reduction causes continuous growth of the initial gold nanoparticles.

The fact that the presence of Au NPs at pH 5 contributes significantly to the kinetics of $AuCl_4^-$ reduction suggests that Au NPs act as mediators that transfer electrons from lactose through CDH to the chloroaurate ions (Figure 5). In other words, it seems that CDH is capable of DET with Au NPs in solution. The Au NP acts as an electron mediator, which transfers the charge to the $AuCl_4^-$. Hence, DET from CDH to Au NP through the heme moiety is a plausible pathway due to the position of this domain at the margins of the protein packaging and its polarity at this pH.[26]

Application of metal nanoparticles as catalysts in biological and biomimetic systems is well documented. The control of their size, structure and composition enables fine-tuning of their physical and chemical properties and therefore integration into biological constituents. Nanoparticles have been applied as nanoconducting elements for enhancing electron transfer between active domains in enzymes or proteins and electrode surfaces.[7a,c,d,23]. Gold nanoparticles have been used extensively for the design of different biosensors.[7f,9d,23d,24] Moreover, numerous studies have demonstrated the ability of Au NPs to wire enzymes to an electrode surface, allowing direct electron transfer .[25] For example, Willner and co-workers designed a neurotransmitter biosensor based on induced growth of Au NPs seeds by tyrosinase.[7a]

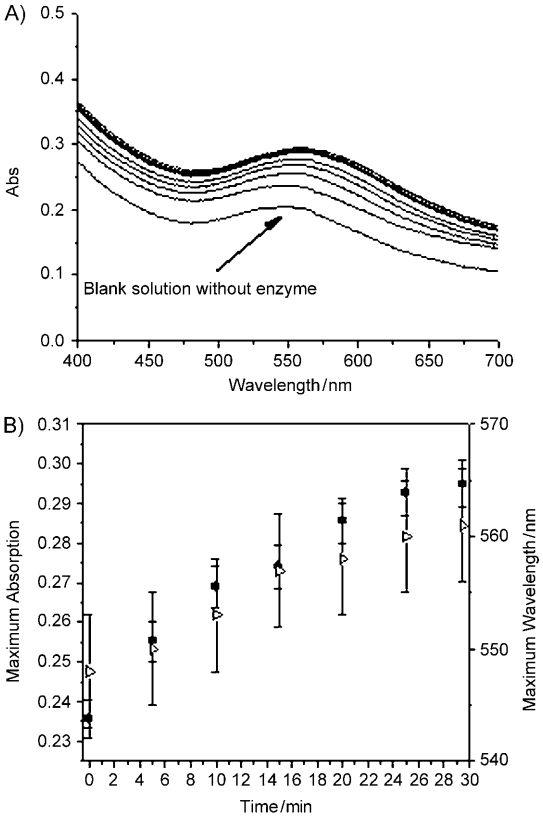


Figure 4. Gold nanoparticle absorption at pH 5. A) Absorption spectra of the reaction solution which contained 0.3 mM β-D-lactose, 0.3 mM $AuCl_4H$ and 25.8 U mL$^{-1}$ CDH catalyzed by 8 nm Au NPs. Interval between runs 5 min. B) Absorption spectra as a function of time showing the absorption maxima (●) and shift in maximum wavelength (▷).

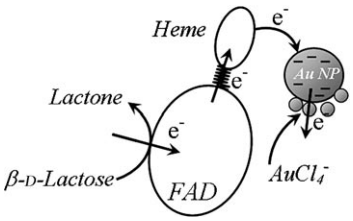


Figure 5. Schematic of DET between CDH and Au NP seed.

Adding BQ (0.3 mM) to the solution consisting of lactose, CDH and Au NPs at pH 5 led to a much faster reaction (Figure 6). The absorption maximum grew much faster until it levelled off after 6 min (instead of 25 min in the absence of BQ). Similarly, the fast change in the absorption wavelength maximum reached a plateau after 6 min, was red-shifted again after 12 min and reached an absorption maximum at 557 nm after 20 min. The simultaneous changes in absorption and wavelength indicate efficient particle

  

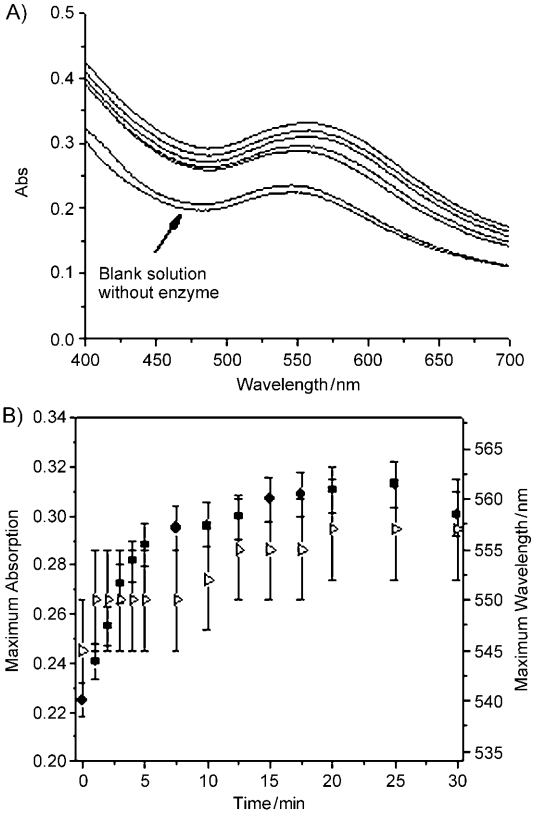


Figure 6. Gold nanoparticle absorption at pH 5. A) Absorption spectra of the reaction solution that contained 0.3 mM β-D-lactose, 0.3 mM BQ, 0.3 mM $AuCl_4H$ and 25.8 U mL$^{-1}$ CDH, catalyzed by adding 8 nm Au NPs. Interval between runs 5 min. B) Absorption spectra as function of time showing the absorption maxima (●) and shift in maximum wavelength (▷).

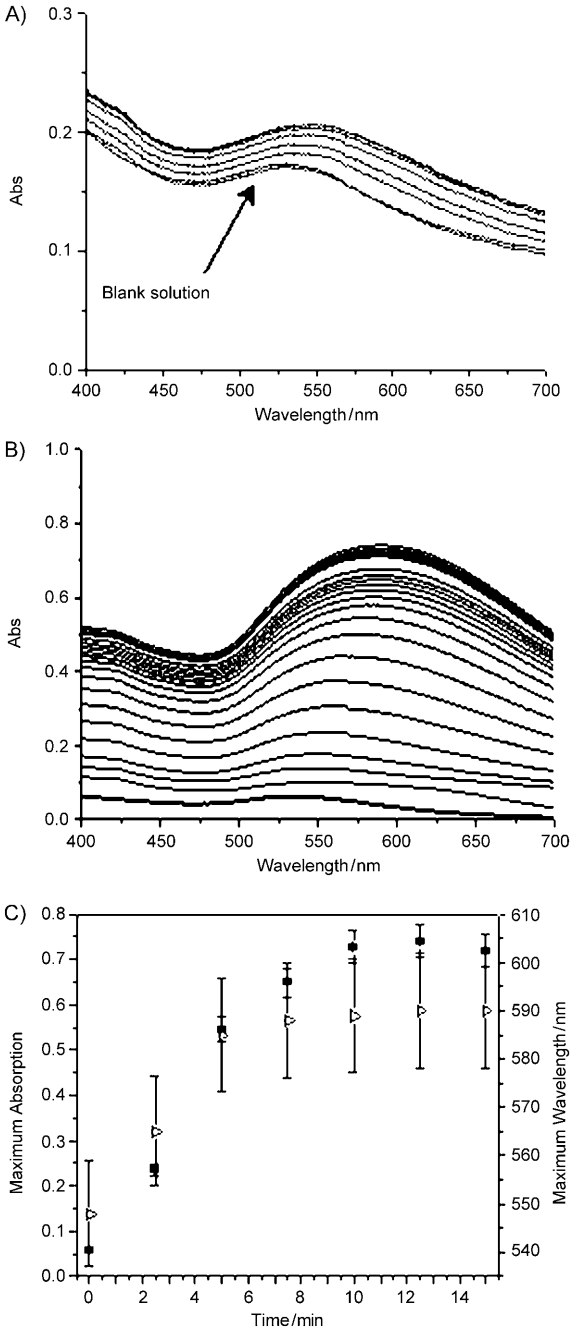


Figure 7. Gold nanoparticle absorption at pH 7. A) Absorption spectra of the reaction solution that contained: 0.3 mM β-D-lactose, 0.3 mM $AuCl_4H$ and 58.2 U mL$^{-1}$ CDH, catalyzed by adding 8 nm Au NPs. Interval between runs 5 min. B) Absorption spectra of the reaction solution A) that also contained 0.3 mM BQ. Interval between runs 30 s. C) Absorption spectra as function of time of graph B), showing the absorption maxima (●) and shift in maximum wavelength (▷).

growth. The fast change in wavelength and absorption (first 6 min) can be explained by rapid Au NP growth. We speculate that this fast process is driven by the MET process through reduction of BQ to $H_2Q$, whereas the second process (12–20 min) is the result of DET between lactose and the Au NPs catalyzed by CDH.

Regeneration of BQ by $AuCl_4^-$ reduction was also investigated. For this, we used catalytic amounts of BQ ($3\times10^{-5}$ M) to assure that it was the limiting reactant in the enzymatic reaction. The set of experiments was carried out at pH 7. It was found (not shown) that the reaction terminated shortly after injection of CDH (58.2 U mL$^{-1}$) into the solution (0.3 mM β-D-lactose, 0.3 mM $AuCl_4^-$, $3\times10^{-5}$ M BQ) with a slight change in absorption due to Au NP formation. This clearly indicates that BQ is not regenerated by reduction of $AuCl_4^-$.

We conducted similar experiments to those shown in Figure 6 but at pH 7, where the role of BQ and therefore the mechanism of $AuCl_4^-$ reduction were elucidated. Figure 7 A shows the change of absorbance in a BQ-free solution upon adding CDH to a solution consisting of $AuCl_4^-$ (0.3 mM), β-D-lactose (0.3 mM) and Au NPs (8 nm diameter). Only a minute change in absorbance could be detected after 30 min, and this suggests that DET is not dominant under these conditions. This is in accordance with previous studies by Gorton et al.,[18–19,26a] who showed that ET between the enzyme domains is blocked at pH 7 and therefore no DET can take place. The change in pH affects the enzyme conformation due to electrostatic repulsion between the different domains, which increases their separation and diminishes

  

the possibility of intramolecular ET.[25a,27] On the other hand, a rapid change in absorbance (Figure 7B) can clearly be seen upon adding BQ (0.3 mM) to the same solution. Figure 7C shows the change in absorbance and wavelength as a function of time (taken from Figure 7B). The absorption grows rapidly and reaches a plateau after 10 min, although the maximum particle growth reached its highest value after 5 min. While the change of absorption is the result of two processes, namely, nucleation and growth, the change in absorption maximum is affected only by the growth. Thus, we can conclude that nucleation proceeds after growth of the NPs has ceased. Clearly, the rate of growth in the presence of Au NPs is much faster than the rate of nucleation, and therefore nucleation continues until the particles have reached their maximum size. The nanoparticle size greatly affects the NP–protein complex activity.[28] Large NPs could lead to protein denaturation ending the deposition process on the Au seeds.[23b]

**Localized deposition of gold nanoparticles by biocatalytic methods**: After studying the reduction of $AuCl_4^-$ catalyzed by CDH, we now aimed at local deposition of gold nanoparticles by SECM. Two basic approaches could be used (Figure 8). In the first approach (Figure 8A) gold ions generated by anodic dissolution of an Au ultra-micro-electrode (UME) are reduced by a mediator (e.g., $H_2Q$) in close proximity to a catalytic substrate such as Pd. The reduced mediator, $H_2Q$, is generated in situ through oxidation of β-D-lactose catalyzed by CDH. In the second, mediatorless approach (Figure 8B) reduction of metal ions occurs by direct electron transfer from the enzyme involving a catalytic surface.

A 25 μm-diameter Au microelectrode was brought close to a Pd surface by following the negative feedback current of oxygen reduction.[10g,29] Once the microelectrode was a few micrometers from the surface, it was stopped and pulsed for different times varying from 1 to 10 s. Another set of experiments involved 1–5 pulses for 1–10 s.

As described above, MET allows fast gold reduction on catalytic substrates at pH 7. Our attempts to locally deposit Au particles by the MET approach (Figure 8A) failed, that is, no deposition of Au was observed. This was surprising recalling that the same system yielded Au NPs in homogenous solution. A possible explanation for the failure to locally deposit Au NPs by the MET approach of SECM can be found in the application of a negative potential (−0.75 V for oxygen reduction) at the tip for approaching

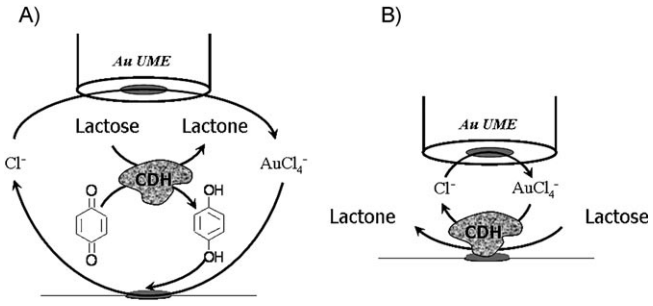


Figure 8. Schematic representations of the two approaches for the localized electroless deposition of Au A) MET biocatalyzed deposition and B) DET biocatalyzed mediatorless deposition of Au NPs.

to the surface.[30] This potential is sufficient to reduce BQ to $H_2Q$, which reacts with BQ in solution producing insoluble oligomers that are absorbed onto the Au microelectrode and block it.[9d,22a] Indeed, we observed a continuous decrease of the feedback current at the tip even when the microelectrode was held at constant distance from the surface.

Hence, we examined the second, mediatorless approach at pH 5, which is optimal for DET. Gold deposition was carried out at different β-D-lactose concentrations (0.3, 3 and 30 mM). Higher sugar concentrations were capable of reducing $AuCl_4^-$ spontaneously (in the absence of a catalyst). Figure 9 shows SEM images of localized gold deposition by SECM in a solution containing β-D-lactose (0.3 mM). To obtain Au deposition the microelectrode was brought close to a Pd surface (1.2 ± 0.5 μm). The gold ions were generated by applying a positive potential (1.35 V) as described above. The substrate–microelectrode distance is a key parameter in successfully depositing Au by CDH. At distances larger than 2 μm no deposition was detected even at higher β-D-lactose concentrations. On the other hand, pulsing the Au microelectrode close enough resulted in clear formation of local-

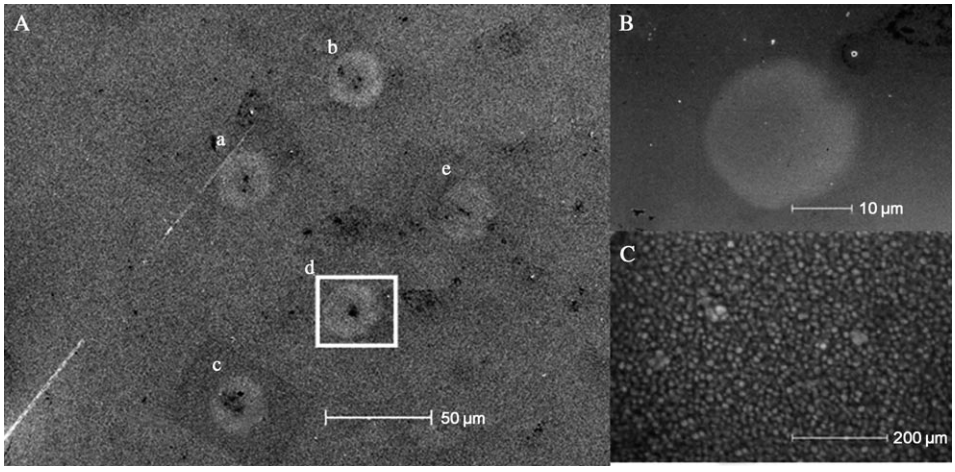


Figure 9. SEM images of localized deposition of Au by SECM applying different deposition times and pulses. A) a) 5 pulses, $t_{dep}$ = 1 s, b) 3 pulses, $t_{dep}$ = 5 s, c) 5 pulses, $t_{dep}$ = 5 s, d) 3 pulses, $t_{dep}$ = 10 s, e) 5 pulses, $t_{dep}$ = 10 s. B) and C) Magnification of spot d). General conditions: β-D-lactose 0.3 mM, KCl 20 mM, buffer phosphate 20 mM pH 5, CDH 25.8 U mL$^{-1}$.

  

ized Au spots and nanostructures (Figure 9). However, at a β-D-lactose concentration of 0.3 mM no deposition of Au could be found for a single pulse (1, 5, 10 s). It seems that gold deposition is not sufficiently fast and presumably requires the formation of some small Au nuclei for massive deposition.

When the pulses were repeated successively at the same spot a characteristic disc-shaped Au deposit was obtained. The shape of the deposited spot matched perfectly the cross-section of the Au microelectrode. Magnifying the micrometer spots (Figure 9B and C) revealed that they are made of nanoparticles with an average diameter of $12\pm3$ nm. Figure 9 shows that neither the duration of the anodic pulse nor the number of pulses significantly affected the size and density of the deposited gold structures under these experimental conditions (0.3 mM β-D-lactose). For example, the diameter of the spots varied by only by 2–3 μm on increasing the pulse duration between 1 and 10 s. Clearly, if diffusion were the rate-limiting step of deposition, we would anticipate that the diameter of the deposited spots would grow linearly with the square root of the anodic pulse duration. Moreover, we did not find any significant effect of the number of pulses and their duration on the nanostructured deposits. This suggests that the concentration of β-D-lactose dictates the amount of gold that is deposited.

Therefore, we decided to carry out the same set of experiments with a higher concentration of β-D-lactose. Increasing the sugar concentration tenfold allowed deposition to be detected after a single pulse, but it had no major effect on the size and density of the deposits. Figure 10 shows the localized deposition of Au with β-D-lactose (30 mM). Now, the number of pulses and their duration had a significant effect on the deposition.

In essence, increasing the number of pulses increased the density of the deposited nanoparticles, although the average particle size remained unchanged. On the other hand, extending the duration of the pulse increases the average size of the Au nanostructures, as can be seen in Figure 11. Extending the duration of five consecutive pulses from 1 to 10 s increased the average diameter of the Au nanoparticles from $10\pm2$ to $40\pm11$ nm.

At concentrations of β-D-lactose greater than 30 mM reduction of gold by the sugar on a catalytic surface (e.g., Au NPs) proceeds spontaneously. When working with 30 mM lactose concentration minute deposition is seen in the absence of CDH. This could imply that the enzyme is not es-

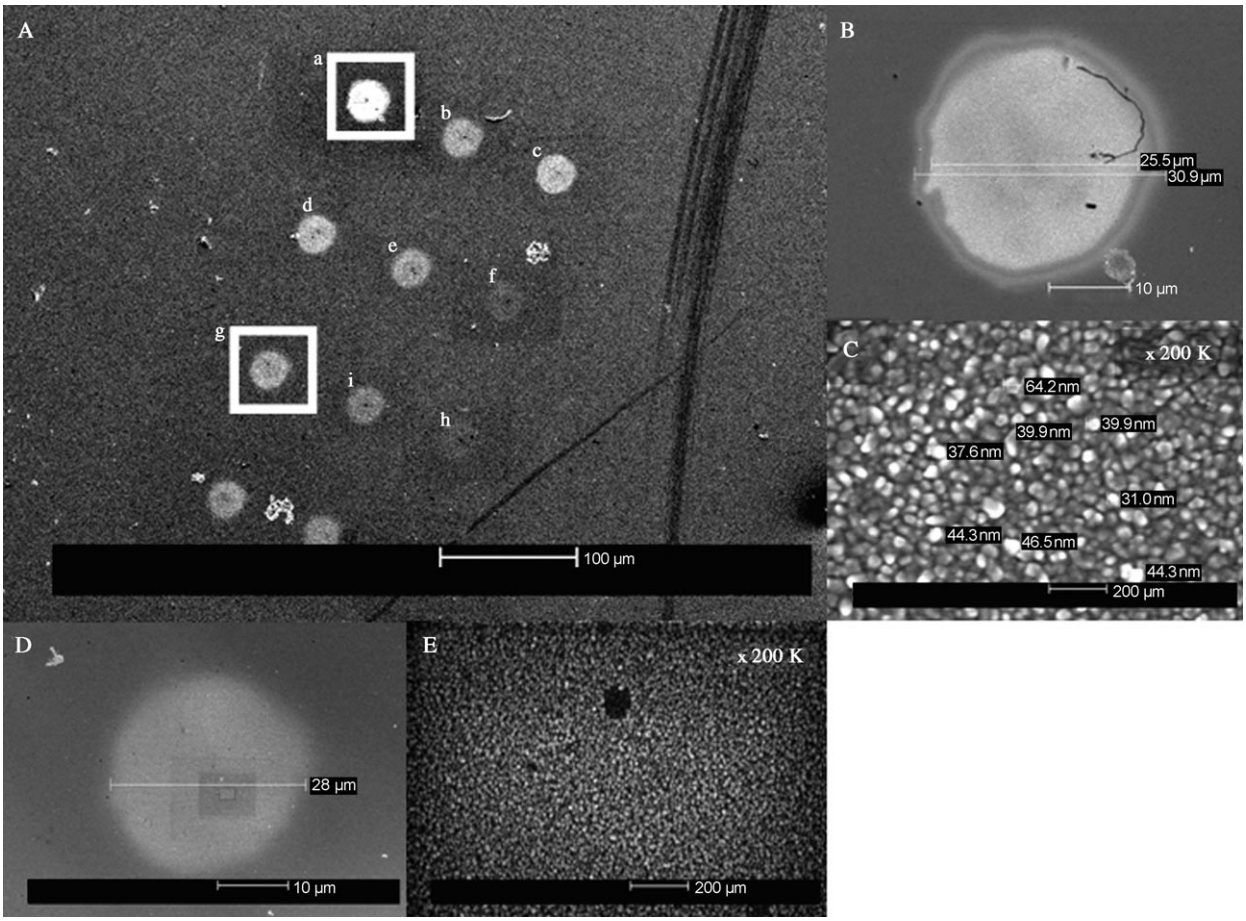


Figure 10. SEM images of Au locally deposited by SECM at different deposition times and pulses. A) a) 5 pulses, $t_{dep}=10$ s, b) 3 pulses, $t_{dep}=10$ s, c) 1 pulse, $t_{dep}=10$ s, d) 5 pulses, $t_{dep}=5$ s, e) 3 pulses, $t_{dep}=5$ s. f) 1 pulse $t_{dep}=5$ s, g) 5 pulses, $t_{dep}=1$ s, h) 3 pulses, $t_{dep}=1$ s, i) 5 pulses, $t_{dep}=1$ s. B) and C) and D) and E) are magnified images of spots a) and g), respectively. [β-D-lactose] was 30 mM, all other conditions are as in Figure 9.

  

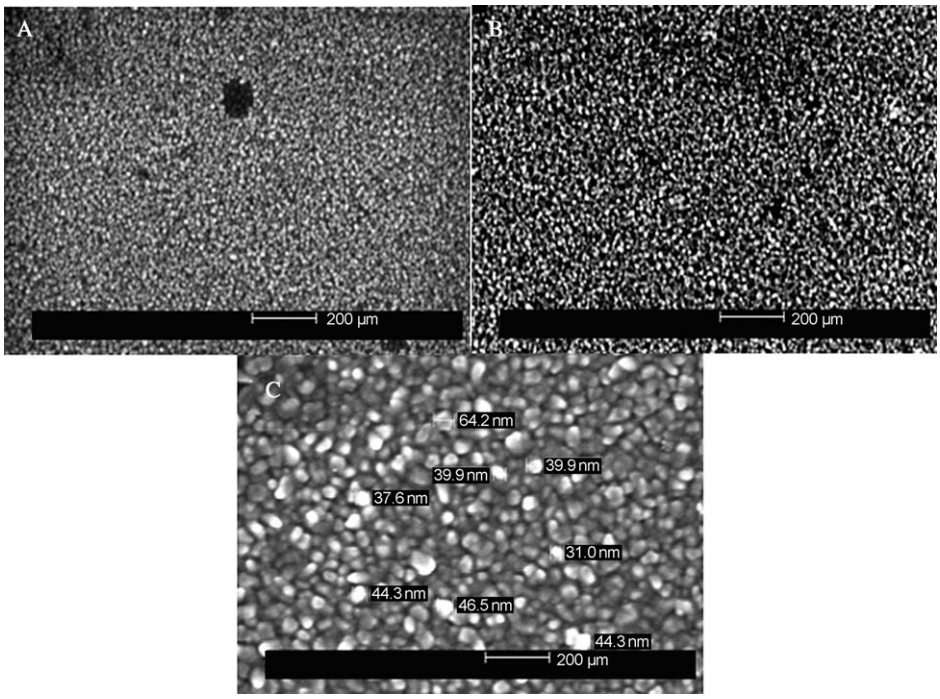


Figure 11. SEM images of Au nanoparticles locally deposited by SECM as a result of five successive pulses of A) 1, B) 5, and C) 10 s. All other parameters are as in Figure 10.

sential for $AuCl_4^-$ reduction. Yet, at lower concentrations of β-D-lactose and in the absence of CDH, $AuCl_4^-$ reduction was not observed. Moreover, in SECM experiments increasing the lactose concentration (from 0.3 to 3 mM) had no influence whatsoever on the deposition characteristics, density or size of the nanostructures. In such case CDH is the main factor in Au deposition. The fact that in 3 mM lactose a single pulse also resulted in gold deposition can be explained by the availability of a higher flux of charge due to higher sugar concentration. Layer-by-layer deposition, in which the number of active sites in the surface increases after each deposition, and instantaneous nucleation and growth can explain Au NP deposition at lower sugar concentrations. We expect that increasing the pulse length and its repetition will increase the size of the deposited particles, as was observed in solution (from the change in spectra), where the particles continue to grow after several minutes. This effect was observed only at 30 mM of β-D-lactose. It could be speculated that at lower sugar concentration, the amount of β-D-lactose under the electrode is rapidly consumed and its diffusion from the bulk is not sufficiently high to maintain the reaction. Moreover, it is plausible that in 30 mM β-D-lactose two processes take place simultaneously, namely, initial reduction of $AuCl_4^-$ on the Pd surface catalyzed by CDH and slow particle growth due to the non-enzymatic reaction between lactose and $AuCl_4^-$ in solution. As mentioned above, it is well known that the interaction between enzyme and NP is greatly affected by the NP dimensions.[31] This fact could explain the results obtained at higher sugar concentrations, in which an increase in Au NP dimensions was seen upon increasing the deposition time. This effect can in particular be noticed in Figure 10 (also in Figure 9a, d and g). We could hypothesize that a threshold size of Au particle is necessary for efficient ET when the enzyme is adsorbed onto the nanoparticle surface. Combining these effects could result in a substantial increase in Au NPs size when a minimum particle radius is reached, as biocatalyzed gold deposition is aided by electroless deposition, such as the reaction observed under 30 mM lactose in the solution.

## Conclusion

Biocatalyzed deposition of Au nanoparticles was demonstrated. We found that direct electron transfer between cellobiose dehydrogenase and Au nanoparticles is not only plausible, but is essential for achieving Au deposition.

The enzyme-catalyzed reduction of $AuCl_4^-$ was accomplished through different paths. The pH-tuneable characteristics of CDH make it possible to form gold nanoparticles in solution by mediated (pH 7) and direct electron transfer (pH 5). At pH 5 $AuCl_4^-$ reduction takes place in the presence of a catalytic surface (e.g., Au NPs). The nanoparticles act as an electron mediator, which transfers the charge from the enzyme to the gold ion. Under these conditions rapid particle growth can be detected by the change in the solution absorption and red-shift of the absorption maxima.

Localized biocatalyzed deposition of Au NPs by scanning electrochemical microscopy was achieved at pH 5. The main factors affecting deposition are the distance between the microelectrode and surface and the β-D-lactose concentration, both of which play an important role in the characteristics of the deposited gold nanoparticles. At low β-D-lactose concentrations the Au nanostructure is affected by the number of pulses but not their duration. The former increases particle density, whereas the latter does not affect the average size of the gold nanoparticles. It could be speculated that under these conditions the limiting factor for nanoparticle growth is the ability of the CDH to interact with the growing Au NPs. At high β-D-lactose concentrations two processes take place: initial Au reduction by CDH on Pd followed by slow particle growth under high sugar concentrations. Under these conditions the deposition time has a major impact on nanoparticle size.

  

## Experimental Section

Electrochemical measurements were conducted by a PC-controlled CHI-750B electrochemical workstation bipotensiostat (CH Instruments Inc., USA) with a rotating disc electrode (RDE) system (EG&G Princeton Applied Research, Model 636). The Scheme of the SECM used in the experiments has been previously described.[29,32] The SECM tip (25 μm diameter Pt disc) was positioned by using miniature linear-stage stepper motors (MFA-PP NewPort Corp. USA) with a resolution of 0.075 μm. The actuators mounted in a *Z–Y* configuration were controlled by a NewPort MM2500 motion controller. The SECM apparatus was placed in a grounded home-made Faraday cage.

Images of the deposited structures were acquired by high-resolution scanning electron microscopy (HRSEM Sirion, FEI Company, USA). UV/Vis experiments were carried out on a Cary 100 Bio spectrophotometer (Varian, Australia).

All reagents and solvents were of the highest commercial quality and were used without further purification. Cellobiose dehydrogenase (CDH) from *Myriococcum thermophilum* CBS 208.89 was grown in submersed culture in shaking flasks and purified to homogeneity according to a previously published method.[19a] The purified enzyme solution had a volumetric activity of 63 $U\,mL^{-1}$ and a specific activity of 3.71 $U\,mg^{-1}$. The activity was measured with 500 μM BQ ($\varepsilon_{290}=2.24\ mM^{-1}\,cm^{-1}$) as electron acceptor and 30 mM lactose as electron donor in 50 mM phosphate buffer (pH 7.0) at 30 °C. At pH 5.0 the volumetric and specific activity was down to 47 % (29 $U\,mL^{-1}$ and 1.71 $U\,mg^{-1}$, respectively).

Preliminary studies on the system were performed by cyclic voltammetry (CV) in a 10 mL electrochemical cell with a standard gold disc electrode (2 mm diameter, CH Instruments Inc. USA) as working electrode, Pt wire as counter-electrode and an Ag|AgCl (KCl saturated) reference electrode. In a typical experiment 0.3 mM BQ and 0.02 M buffer phosphate (pH 7.0) were added to the electrochemical cell and deaerated for 5 min with $N_2$ flow. A CV was then recorded (0.4 V to −0.1 V at 100 $mV\,s^{-1}$). In a similar manner the electrochemical behavior of β-D-lactose, and CDH was studied.

CDH activity was determined at different pH by chronoamperometry with β-D-lactose as electron donor and BQ as electron acceptor. Typically, the RDE was rotated (1500 rpm) in a solution containing 0.3 mM β-D-lactose, 0.3 mM BQ and buffer. After 100 s a known amount of CDH was injected into the cell and the $H_2Q$ produced was oxidized to BQ by applying a constant potential of 0.3 V versus Ag|AgCl.

SECM experiments were carried out with an Ag|AgCl quasi-reference electrode (QRE) and a Pt wire as counter-electrode. A Pd substrate was immersed in the deposition bath containing 20 mM KCl, β-D-lactose at different concentrations, buffer phosphate 20 mM (pH 5) and CDH (0.32 U). Gold deposition on the Pd surface was carried out by approaching the substrate with the Au ultra-micro-electrode ($E_{tip}=-0.75$ V at pH 5.0) and following the negative feedback current due to oxygen reduction.[30] The exact tip–surface distance was determined by fitting the approaching curve with the theoretical negative feedback current.[9c] Once the tip was positioned a few micrometers above the surface a series of anodic potential pulses (5–10 s each) was applied to the Au tip to generate a flux of $AuCl_4^-$ ions. These pulses were repeated at different locations (while maintaining the same distance from the surface) or upon changing the length of the pulse or the number of pulses applied at the same location.

## Acknowledgements

This work was supported by the Israel Science Foundation (contract 485-06). The Harvey M. Krueger Family Centre for Nanoscience and Nanotechnology of the Hebrew University is acknowledged. R.L. acknowledges the Austrian Academy of Sciences for financial support (APART 11322). L.G. thanks the Swedish Research Council.

[1] a) J. V. Zoval, R. M. Stiger, P. R. Biernacki, R. M. Penner, *J. Phys. Chem.* **1996**, *100*, 837–844; b) R. Maoz, E. Frydman, S. R. Cohen, J. Sagiv, *Adv. Mater.* **2000**, *12*, 725; c) M. S. El-Deab, T. Sotomura, T. Ohsaka, *J. Electrochem. Soc.* **2005**, *152*, C730–C737; d) M. Palomar-Pardavé, I. Gonzalez, N. Batina, *J. Phys. Chem. B* **2000**, *104*, 3545–3555; e) S. Meltzer, D. Mandler, *J. Electrochem. Soc.* **1995**, *142*, L82L84.

[2] a) B. Basnar, Y. Weizmann, Z. Cheglakov, I. Willner, *Adv. Mater.* **2006**, *18*, 713-; b) T. M. Day, P. R. Unwin, J. V. Macpherson, *Nano Lett.* **2007**, *7*, 51–57; c) J. E. Ghadiali, M. M. Stevens, *Adv. Mater.* **2008**, *20*, 4359–4363; d) S. E. Gilbert, O. Cavalleri, K. Kern, *J. Phys. Chem.* **1996**, *100*, 12123–12130; e) S. Kawabata, Y. Naono, Y. Taguchi, S. H. Huh, A. Nakajima, *Appl. Surface Sci.* **2007**, *253*, 6690–6696.

[3] a) T. S. Ahmadi, Z. L. Wang, T. C. Green, A. Henglein, M. A. El-sayed, *Science* **1996**, *272*, 1924–1926; b) T. Asefa, R. B. Lennox, *Chem. Mater.* **2005**, *17*, 2481–2483; c) K. C. Grabar, R. G. Freeman, M. B. Hommer, M. J. Natan, *Anal. Chem.* **1995**, *67*, 735–743; d) Z. Q. Peng, L. M. Guo, Z. H. Zhang, B. Tesche, T. Wilke, D. Ogermann, S. H. Hu, K. Kleinermanns, *Langmuir* **2006**, *22*, 10915–10918; e) Z. L. Wang, M. B. Mohamed, S. Link, M. A. El-Sayed, *Surfactant Sci. Ser.* **1999**, *440*, L809–L814.

[4] a) S. J. Clarson, P. W. Whitlock, S. V. Patwardhan, L. L. Brott, R. R. Naik, M. O. Stone, *Abstr. Pap. Am. Chem. Soc.* **2002**, *223*, 231; b) Y. Xiao, B. Shlyahovsky, I. Popov, V. Pavlov, I. Willner, *Langmuir* **2005**, *21*, 5659–5662; c) T. Yang, Z. Li, L. Wang, C. L. Guo, Y. J. Sun, *Langmuir* **2007**, *23*, 10533–10538.

[5] a) R. R. Naik, S. J. Stringer, G. Agarwal, S. E. Jones, M. O. Stone, *Nat. Mater.* **2002**, *1*, 169–172; b) S. L. Sewell, D. W. Wright, *Chem. Mater.* **2006**, *18*, 3108–3113.

[6] a) E. Kharlampieva, J. M. Slocik, T. Tsukruk, R. R. Naik, V. V. Tsukruk, *Chem. Mater.* **2008**, *20*, 5822–5831; b) E. Kharlampieva, T. Tsukruk, J. M. Slocik, H. Ko, N. Poulsen, R. R. Naik, N. Kroger, V. V. Tsukruk, *Adv. Mater.* **2008**, *20*, 3274-; c) E. Kharlampieva, D. Zimnitsky, M. Gupta, K. N. Bergman, D. L. Kaplan, R. R. Naik, V. V. Tsukruk, *Chem. Mater.* **2009**, *21*, 2696–2704; d) M. Umetsu, M. Mizuta, K. Tsumoto, S. Ohara, S. Takami, H. Watanabe, I. Kumagai, T. Adschiri, *Adv. Mater.* **2005**, *17*, 2571–2575.

[7] a) R. Baron, M. Zayats, I. Willner, *Anal. Chem.* **2005**, *77*, 1566–1571; b) I. Willner, R. Baron, B. Willner, *Biosens. Bioelectron.* **2007**, *22*, 1841–1852; c) I. Willner, R. Baron, B. Willner, *Adv. Mater.* **2006**, *18*, 1109–1120; d) M. Zayats, R. Baron, I. Popov, I. Willner, *Nano Lett.* **2005**, *5*, 21–25; e) B. K. Jena, C. R. Raj, *Electroanalysis* **2007**, *19*, 816–822; f) J. M. Pingarron, P. Yanez-Sedeno, A. Gonzalez-Cortes, *Electrochim. Acta* **2008**, *53*, 5848–5866.

[8] X. Luo, V. Pedrosa, J. Wang, *Chem. Eur. J.* **2009**, *15*, 5191–5194.

[9] a) M. Arca, M. V. Mirkin, A. J. Bard, *J. Phys. Chem.* **1995**, *99*, 5040–5050; b) A. J. Bard, M. V. Mirkin, P. R. Unwin, D. O. Wipf, *J. Phys. Chem.* **1992**, *96*, 1861–1868; c) J. Kwak, A. J. Bard, *Anal. Chem.* **1989**, *61*, 1221–1227; d) K. T. Lau, S. A. L. De Fortescu, L. J. Murphy, J. M. Slater, *Electroanalysis* **2003**, *15*, 975–981; e) D. Mandler, A. J. Bard, *J. Electrochem. Soc.* **1989**, *136*, 3143–3144; f) G. Nagy, L. Nagy, *Fresenius J. Anal. Chem.* **2000**, *366*, 735–744; g) P. R. Unwin, A. J. Bard, *J. Phys. Chem.* **1991**, *95*, 7814–7824; h) A. L. Whitworth, D. Mandler, P. R. Unwin, *Phys. Chem. Chem. Phys.* **2005**, *7*, 356–365; i) G. Wittstock, B. Grundig, B. Strehlitz, K. Zimmer, *Electroanalysis* **1998**, *10*, 526–531.

[10] a) C. Combellas, F. Kanoufi, D. Mazouzi, A. Thiebault, *J. Electroanal. Chem.* **2003**, *556*, 43–52; b) O. De Abril, D. Mandler, P. R. Unwin, *Electrochem. Solid-State Lett.* **2004**, *7*, C71-C74; c) C. Hess, K. Borgwarth, C. Ricken, D. G. Ebling, J. Heinze, *Electrochim. Acta* **1997**, *42*, 3065–3073; d) E. Malel, D. Mandler, *J. Electrochem. Soc.* **2008**, *155*, D459-D467; e) A. K. Neufeld, A. P. O'mullane, A. M. Bond, *J. Am. Chem. Soc.* **2005**, *127*, 13846–13853; f) M. Sheffer, D. Mandler, *J. Electrochem. Soc.* **2008**, *155*, D203-D208; g) P. R. Unwin, J. V. Macpherson, R. D. Martin, C. F. McConville in *Electrochemical Microscopy as a Dynamic Probe of Metal Adsorption, Nucleation and Growth on Surfaces: Silver Deposition on Pyrite* (Eds.:

  

S. R. Taylor, A. C. Hillier, M. Seo), The Electrochemical Society, New Jersey, **2000**.
[11] a) E. Ammann, D. Mandler, *J. Electrochem. Soc.* **2001**, *148*, C533-C539; b) K. Borgwarth, J. Heinze, *J. Electrochem. Soc.* **1999**, *146*, 3285–3289; c) T. Danieli, N. Gaponik, A. Eychmuller, D. Mandler, *J. Phys. Chem. C* **2008**, *112*, 8881–8889.
[12] L. Stoica, A. Lindgren-Sjölander, T. Ruzgas, L. Gorton, *Anal. Chem.* **2004**, *76*, 4690–4696.
[13] L. Stoica, T. Ruzgas, R. Ludwig, D. Haltrich, L. Gorton, *Langmuir* **2006**, *22*, 10801–10806.
[14] M. R. Coudray, G. Canevascini, H. Meier, *Biochem. J.* **1982**, *203*, 277–284.
[15] a) S. S. Subramaniam, S. R. Nagalla, V. Renganathan, *Arch. Biochem. Biophys.* **1999**, *365*, 223–230; b) R. Ludwig, W. Harreither, F. Tasca, L. Gorton, *ChemPhysChem*, **2010**, *11*, 2674,–2697.
[16] a) T. Larsson, A. Lindgren, T. Ruzgas, S. E. Lindquist, L. Gorton, *J. Electroanal. Chem.* **2000**, *482*, 1–10; b) A. Lindgren, T. Larsson, T. Ruzgas, L. Gorton, *J. Electroanal. Chem.* **2000**, *494*, 105–113.
[17] F. Tasca, L. Gorton, W. Harreither, D. Haltrich, R. Ludwig, G. Nöll, *J. Phys. Chem. C* **2008**, *112*, 9956–9961.
[18] V. Coman, W. Harreither, R. Ludwig, D. Haltrich, L. Gorton, *Chem. Anal.* **2007**, *52*, 945–960.
[19] a) W. Harreither, V. Coman, R. Ludwig, D. Haltrich, L. Gorton, *Electroanalysis* **2007**, *19*, 172–180; b) L. Stoica, R. Ludwig, D. Haltrich, L. Gorton, *Anal. Chem.* **2006**, *78*, 393–398.
[20] M. Zamocky, R. Ludwig, C. Peterbauer, B. M. Hallberg, C. Divne, P. Nicholls, D. Haltrich, *Curr. Protein Pept. Sci.* **2006**, *7*, 255–280.
[21] S. Link, M. A. El-Sayed, *J. Phys. Chem. B* **1999**, *103*, 8410–8426.
[22] a) S. I. Bailey, I. M. Ritchie, *Electrochim. Acta* **1985**, *30*, 3–12; b) S. I. Bailey, I. M. Ritchie, F. R. Hewgill, *J. Chem. Soc. Perkin Trans. 2* **1983**, 645–652.
[23] a) D. M. Adams, L. Brus, C. E. D. Chidsey, S. Creager, C. Creutz, C. R. Kagan, P. V. Kamat, M. Lieberman, S. Lindsay, R. A. Marcus, R. M. Metzger, M. E. Michel-Beyerle, J. R. Miller, M. D. Newton, D. R. Rolison, O. Sankey, K. S. Schanze, J. Yardley, X. Y. Zhu, *J. Phys. Chem. B* **2003**, *107*, 6668–6697; b) M. E. Aubin-Tam, K. Hamad-Schifferli, *Biomed. Mater.* **2008**, *3*; c) J. Y. Chen, B. Lim, E. P. Lee, Y. N. Xia, *Nano Today* **2009**, *4*, 81–95; d) E. Katz, I. Willner, *Angew. Chem.* **2004**, *116*, 6166–6235; *Angew. Chem. Int. Ed.* **2004**, *43*, 6042–6108; e) X. L. Luo, A. Morrin, A. J. Killard, M. R. Smyth, *Electroanalysis* **2006**, *18*, 319–326; f) C. L. Xiang, Y. J. Zou, L. X. Sun, F. Xu, *Electrochem. Commun.* **2008**, *10*, 38–41.
[24] L. Murphy, *Curr. Opin. Chem. Biol.* **2006**, *10*, 177–184.
[25] a) J. M. Abad, M. Gass, A. Bleloch, D. J. Schiffrin, *J. Am. Chem. Soc.* **2009**, *131*, 10229–10236; b) L. Wang, E. K. Wang, *Electrochem. Commun.* **2004**, *6*, 49–54.
[26] a) F. Tasca, L. Gorton, W. Harreither, D. Haltrich, R. Ludwig, G. Nöll, *Anal. Chem.* **2009**, *81*, 2791–2798; b) A. Lindgren, L. Gorton, T. Ruzgas, U. Baminger, D. Haltrich, M. Schülein, *J. Electroanal. Chem.* **2001**, *496*, 76–81.
[27] M. Zamocky, C. Schumann, C. Sygmund, J. O'Callaghan, A. D. W. Dobson, R. Ludwig, D. Haltrich, C. K. Peterbauer, *Protein Expression Purif.* **2008**, *59*, 258–265.
[28] P. Roach, D. Farrar, C. C. Perry, *J. Am. Chem. Soc.* **2006**, *128*, 3939–3945.
[29] M. Gonsalves, A. L. Barker, J. V. Macpherson, P. R. Unwin, D. O'hare, C. P. Winlove, *Biophys. J.* **2000**, *78*, 1578–1588.
[30] A. Sarapuu, K. Tammeveski, T. T. Tenno, V. Sammelselg, K. Kontturi, D. J. Schiffrin, *Electrochem. Commun.* **2001**, *3*, 446–450.
[31] a) J. Deka, A. Paul, A. Ramesh, A. Chattopadhyay, *Langmuir* **2008**, *24*, 9945–9951; b) S. J. Huo, X. K. Xue, Q. X. Li, S. F. Xu, W. B. Cai, *J. Phys. Chem. B* **2006**, *110*, 25721–25728.
[32] A. J. Bard, F. R. F. Fan, J. Kwak, O. Lev, *Anal. Chem.* **1989**, *61*, 132–138.

Received: February 20, 2010
Revised: June 14, 2010
Published online: September 6, 2010

  